

Supporting Information

Guest-activated forbidden tilts in a molecular perovskite analogue

Samuel G. Duyker,^{*,a,b} Joshua A. Hill,^a Christopher J. Howard,^c and Andrew L. Goodwin^{*,a}

^a Department of Chemistry, University of Oxford, Inorganic Chemistry Laboratory, South Parks Road, Oxford, OX1 3QR, UK

^b School of Chemistry, University of Sydney, Sydney, NSW 2006, Australia

^c School of Engineering, University of Newcastle, Callaghan, NSW 2308, Australia

Experimental Details

Synthesis. Solutions of 2 mmol (568 mg; in excess) $(\text{NH}_4)_4\text{Fe}(\text{CN})_6$ dissolved in 1.5 mL H_2O and 1 mmol (267 mg) $\text{SrCl}_2 \cdot 6\text{H}_2\text{O}$ dissolved in 1.0 mL H_2O were mixed and the mixture left to stand. Faintly green irregular hexagonal crystals of $1 \cdot 2\text{H}_2\text{O}$ formed within 5 minutes.

X-ray single crystal diffraction. X-ray diffraction data from the single crystal were collected using an Oxford Diffraction (Rigaku Oxford Diffraction) SuperNova diffractometer fitted with an Oxford Cryosystems Cryostream 700 Plus open-flow nitrogen cooling device ($\lambda = 1.54184 \text{ \AA}$).³² CrysAlisPro³³ was used for data collection and reduction. The structures were solved *ab initio* using SIR92 with any missing atoms identified in subsequent Fourier difference maps.³⁴ Both structures were refined with full-matrix least-squares on F^2 using CRYSTALS.^{35,36} Hydrogen atoms were, in both cases, visible in the difference Fourier map and treated in the usual manner.³⁷ Full structural data are included in the SI, including CIF files, and have been submitted to the CCDC as numbers 1489336 and 1489337. These data can also be obtained free of charge from The Cambridge Crystallographic Data Centre via http://www.ccdc.cam.ac.uk/data_request/cif.

X-ray powder diffraction. XRPD data were collected for as-synthesized $1 \cdot 2\text{H}_2\text{O}$, dehydrated **1**, and re-hydrated $1 \cdot 2\text{H}_2\text{O}$, with the samples sealed in 0.7 mm diameter glass capillaries for analysis. Dehydration was achieved by applying a vacuum of $\sim 10^{-1}$ mbar at room temperature for 12 h. Rehydration of the sample was carried out by exposing the evacuated sample to pure water vapor in an otherwise evacuated sealed system at room temperature for 12 h. XRPD patterns were obtained in the $10\text{--}50^\circ$ 2θ range using $\text{Cu-K}\alpha$ radiation ($\lambda = 1.5405 \text{ \AA}$) in Debye-Scherrer geometry for 30 min per pattern on a PANalytical X'Pert Pro MPD instrument. Simulated XRPD patterns were generated from the single crystal structures using Mercury.³⁸

Thermogravimetry. Thermogravimetric data were collected for $1 \cdot 2\text{H}_2\text{O}$ on a TA Instruments Discovery TGA thermobalance, under N_2 flow with a heating rate of 100 K min^{-1} from 293 K to 480 K.

Symmetry analysis. Careful analysis of the $1 \cdot 2\text{H}_2\text{O}$ $C2/c$ structure in relation to the $Pm\bar{3}m$ perovskite aristotype determined that the basis vectors relating the latter to the former are $[1 \ 2 \ 1]$, $[-1 \ 0 \ 1]$ and $[1 \ -2 \ 1]$ with the origin at $(0, \frac{1}{2}, \frac{1}{2})$. The ISOTROPY²⁷ software suite was used to identify irrep Λ_3 as sufficient to generate the $C2/c$ structure from the perovskite parent. A mode decomposition analysis was performed by inputting the parent and daughter structures into ISODISTORT to determine the distortion modes and their amplitudes.

(32) Cosier, J.; Glazer, A. M. *J. Appl. Crystallogr.* **1986**, *19*, 105.

(33) CrysAlisPRO, Oxford Diffraction /Agilent Technologies UK Ltd, Yarnton, England.

(34) Altomare, A.; Cascarano, G.; Giacovazzo, C.; Guagliardi, A.; Burla, M. C.; Polidori, G.; Camalli, M. *J. Appl. Crystallogr.* **1994**, *27*, 435.

(35) Betteridge, P. W.; Carruthers, J. R.; Cooper, R. I.; Prout, K.; Watkin, D. J. *J. Appl. Crystallogr.* **2003**, *36*, 1487.

(36) Parois, P.; Cooper, R. I.; Thompson, A. L. *Chem. Cent. J.* **2015**, *9*, 1.

(37) Cooper, R. I.; Thompson, A. L.; Watkin, D. J. *J. Appl. Crystallogr.* **2010**, *43*, 1100.

(38) Macrae, C. F.; Bruno, I. J.; Chisholm, J. A.; Edgington, P. R.; McCabe, P.; Pidcock, E.; Rodriguez-Monge, L.; Taylor, R.; van de Streek, J.; Wood, P. A. *J. Appl. Crystallogr.* **2008**, *41*, 466.

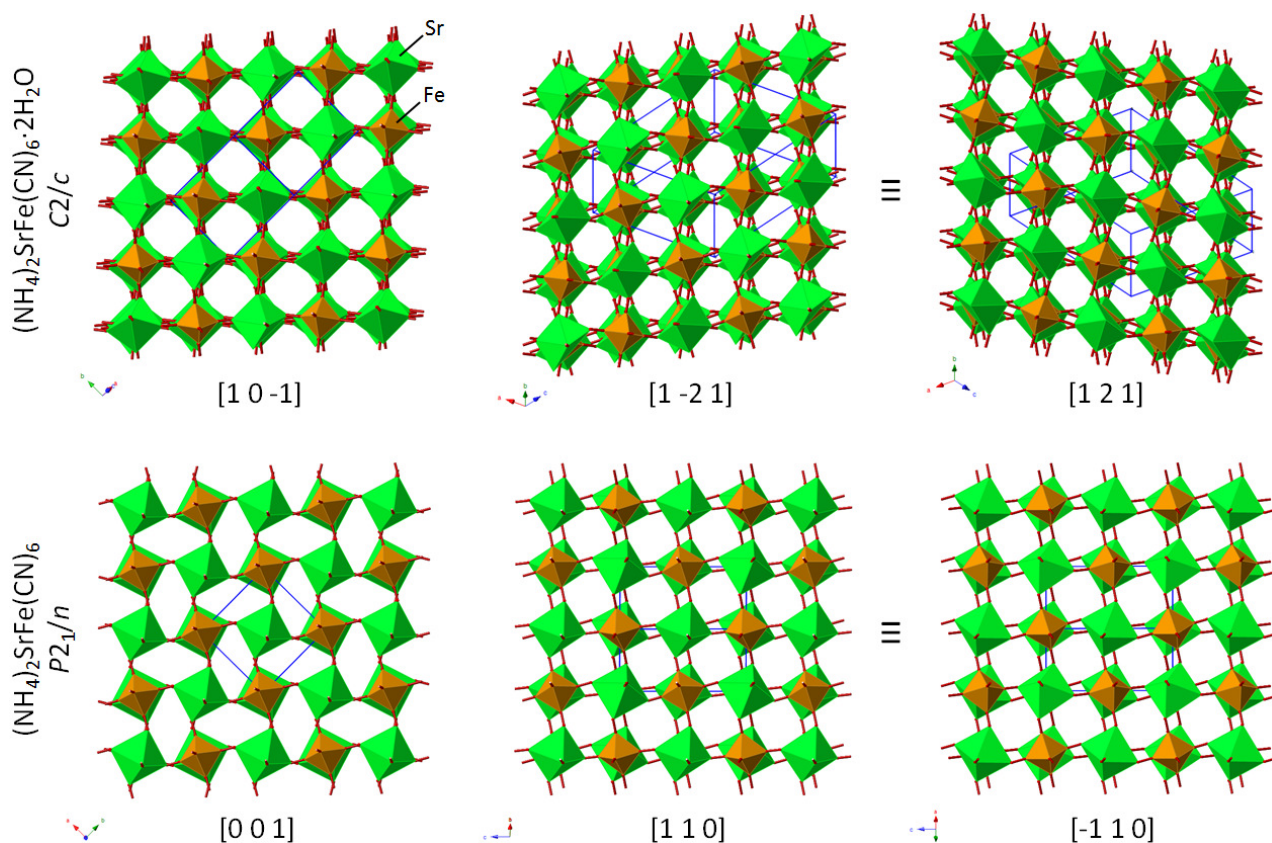


Figure S1. Views showing multiple layers of the $1 \cdot 2\text{H}_2\text{O}$ (top) and 1 (bottom) crystal structures, seen along the three (two unique) perovskite axes of each structure. The Sr polyhedra are shown in green, Fe in orange, cyanide bridges in red. NH_4^+ and H_2O are omitted for clarity.

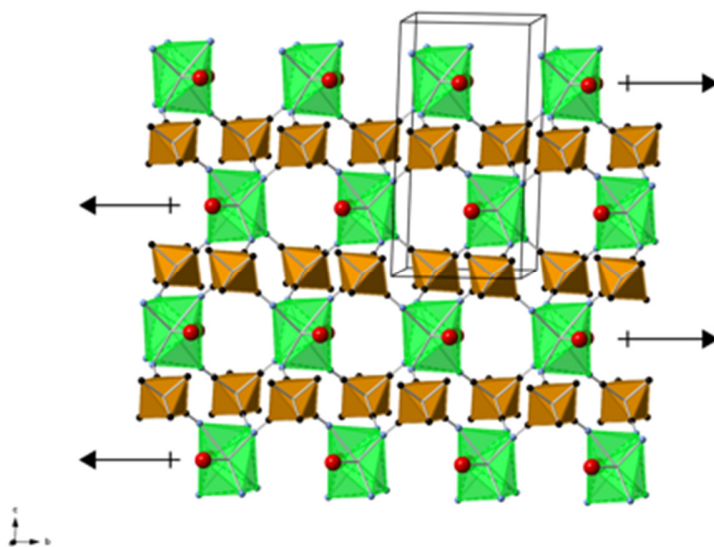


Figure S2. Illustration of the polarization in the Sr layers of the $1 \cdot 2\text{H}_2\text{O}$ structure, generated by the ordering within each layer of the asymmetric H_2O coordination (and resulting local polarization) around each Sr ion. Due to the antiparallel H_2O orientations in neighboring layers, the net polarization is zero.

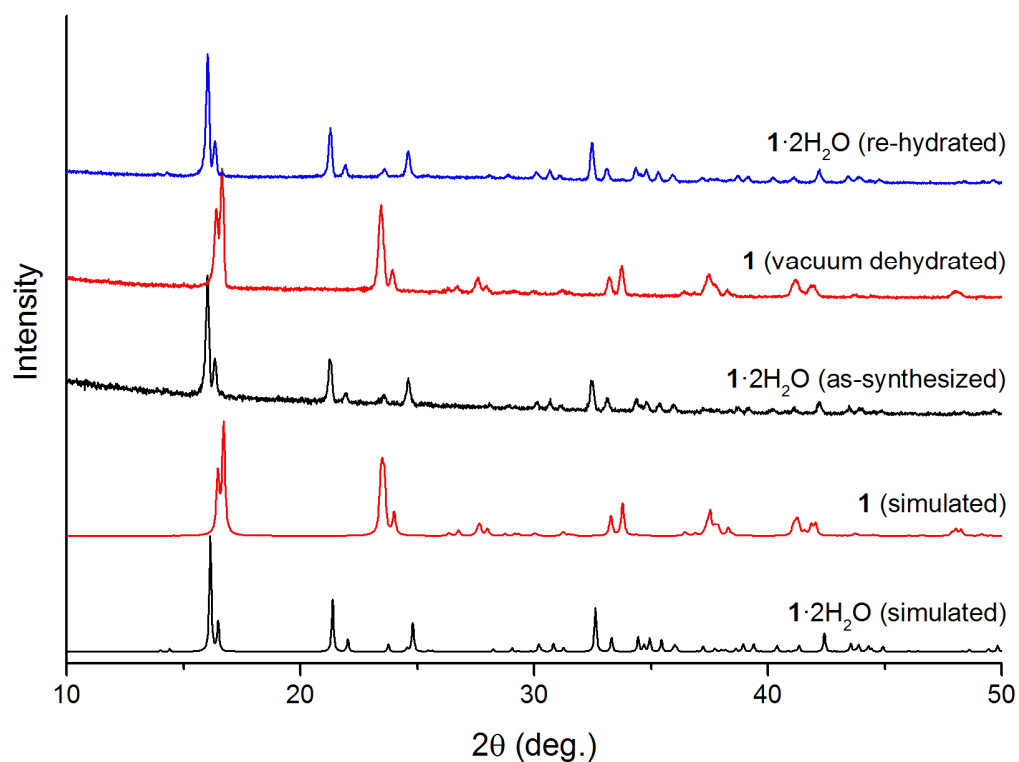


Figure S3. X-ray powder diffraction data for the as-synthesized, dehydrated, and re-hydrated material, showing complete reversibility of the structural conversion observed upon dehydration. The experimental powder patterns show good agreement with those simulated from the single crystal structures.

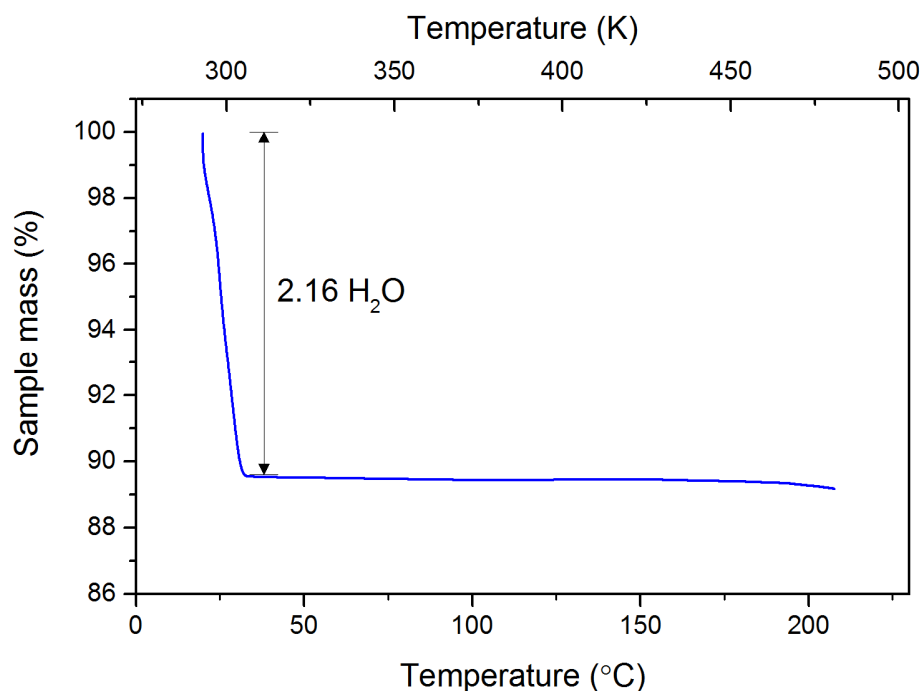


Figure S4. Thermogravimetric data during heating of $1 \cdot 2\text{H}_2\text{O}$ under N_2 flow. Dehydration is complete by 310 K, and thermal decomposition begins at ~ 475 K. The mass loss below 310 K corresponds to removal of 2.16 mol/mol of water from the framework, consistent with a dihydrate compound.